Flowsheet Development and Selective Flotation of Lithium Minerals from the Moose II Pegmatite, Canada

[1,2]Espoir Murhula, [3]Gideon Lambiv Dzemua, [4]Wennie Wang, [1]Levie Mweene, [5]Tassos Grammatikopoulos, [1]Charlotte Gibson

[1]Queen's University, Canada

[2]Critical Minerals Reactivity Lab Inc., Canada

[3]NWT Geological Survey, Canada

[4]The University of Texas at Austin, USA

[5]SGS Natural Resources, Canada

Abstract. This study examines the beneficiation potential of lithium-bearing minerals from the Moose II lithium-cesium-tantalum (LCT) pegmatite in the Northwest Territories, Canada, with a focus on the selective concentration and recovery of montebrasite/amblygonite and spodumene. According to comprehensive mineralogical analyses using TIMA-X, electron microprobe, and laser ablation, the samples in the study contained 7.25% spodumene and 24.5% montebrasite, with both minerals fully liberated below 300 µm. Bench-scale flotation tests were performed to develop a preliminary flowsheet for the recovery of dual lithium minerals. Initial test conditions produced a montebrasite rougher concentrate containing 70.42% of the total lithium, grading 7.52% Li_2O, and a spodumene rougher concentrate containing 12.94% of the lithium, grading 3.10% Li2O, demonstrating potential for lithium recovery from the deposit. Response surface methodology (central composite design) was then used to optimize the selective flotation of montebrasite from spodumene using P_2O_5 and SiO_2 as respective proxies. The results showed that pH was the dominant control on montebrasite recovery and that Na_2CO_3 improves selectivity, with the best operating window at pH 9.50–9.62 and Na_2CO_3 dosages of about 930–1350 g/t. Complementary density functional theory (DFT) calculations and spectroscopy provided new insights into mineral–reagent interactions, enabling understanding of the surface chemistry necessary for separation performance. Integrating mineralogical, flotation, and surface chemistry results provides the first mechanistic understanding of separating montebrasite and spodumene from phosphate-rich LCT pegmatites. These findings provide a basis for optimized flowsheet design for lithium mineral processing from unconventional pegmatite sources.

Keywords: lithium, montebrasite, spodumene, critical minerals, surface chemistry

1 Introduction

Lithium is a critical metal for the energy transition, driven mainly by lithium-ion batteries for electric vehicles and stationary energy storage. Hard-rock lithium-cesium-tantalum (LCT) pegmatites, in which spodumene is the principal ore mineral, are a major source of this supply, and their beneficiation is challenged by the close similarity in physical and chemical properties between lithium minerals and the associated gangue [1–3].

Spodumene and the amblygonite-montebrasite solid solution are the main lithium-bearing minerals in phosphorus-rich (P-rich) LCT pegmatites, and their selective separation is necessary for effective downstream lithium extraction. The Moose II deposit in the Northwest Territories, Canada, is a P-rich pegmatite with abundant spodumene and montebrasite. This pegmatite body is characterized by a variety of textural and paragenetic features and contains a range of economic minerals, including spodumene and montebrasite for lithium, columbite-tantalite for niobium and tantalum, and cassiterite for tin [4]. These valuable minerals occur along with quartz, feldspars, and muscovite as major gangue minerals. The general flowsheet for separating valuable minerals from gangue in pegmatites is well established, with only a few variants. Depending on the mineral assemblage and liberation size, it combines dense media separation and other gravity methods, magnetic separation, and flotation [5]. However, available flowsheets generally do not consider the amblygonite-montebrasite series of minerals. Montebrasite has a higher theoretical lithium content than spodumene (theoretically, 10.2% vs. 8.0% Li_2O) and should therefore be recovered as a product in its own right. Moreover, members of the series contain phosphorus and fluorine, which are deleterious in spodumene concentrate and may complicate the extraction of lithium from spodumene [6]. In this study, the series is referred to as montebrasite, as montebrasite is more common than amblygonite, is fluorine-poor, and is currently gaining more attention from the scientific community as a source of lithium and other critical metals [7,8]. Separating montebrasite from spodumene by flotation is challenging because both minerals respond to the anionic fatty-acid collectors conventionally used for spodumene. Fatty-acid adsorption on spodumene is attributed to chemisorption at exposed Al sites, so its floatability is strongly governed by pulp pH, surface pretreatment such as high-density alkaline conditioning, and activation by metal cations in process water [1,9]. Montebrasite, in contrast, has received little attention; our recent spectroscopic and first-principles work showed that its surface is amphoteric and that it interacts more strongly

with fatty-acid collectors than spodumene does [8,10]. Sodium carbonate, a common pH modifier, has also been shown to alter the flotation response of spodumene [11–13], suggesting that it could be used to tune selectivity between the two lithium minerals. However, no study has yet combined mineralogy, bench-scale flotation, and statistical optimization to define the conditions for separating montebrasite from spodumene in a natural pegmatite ore.

With the Moose II pegmatite as a case study, this study aims to develop a preliminary flowsheet for the recovery of both lithium minerals. Specifically, we (i) characterize the mineralogy, liberation, and lithium content of the lithium minerals; (ii) evaluate a sequential mica–montebrasite–spodumene flotation scheme at bench scale; and (iii) use response surface methodology to quantify the effects of pH and Na_2CO_3 dosage on the selective flotation of montebrasite from spodumene, using P_2O_5 and SiO_2 recoveries, the Gaudin selectivity index, and separation efficiency as responses. The results will support the development of phosphate-rich LCT pegmatites, adding value by recovering lithium phosphate minerals as a separate product.

2 Methods

2.1 Sample preparation and characterization

The sample was crushed to -3 mm stage-ground to 100% 300 µm, and then rotary split into representative charges of 2 kg each, from which 2 random charges were subjected to size analysis (Figure 1). Representative sub-samples were collected and analyzed using TIMA-X to assess mineral liberation (SGS in Lakefield, ON); electron microprobe to determine the iron content of lithium minerals; and laser ablation to establish the lithium content of spodumene and montebrasite (EPMA and LA at Queen's University). The head grade, from EPMA-LA-ICP-MS, was assay at 2.72 % Li_2O.

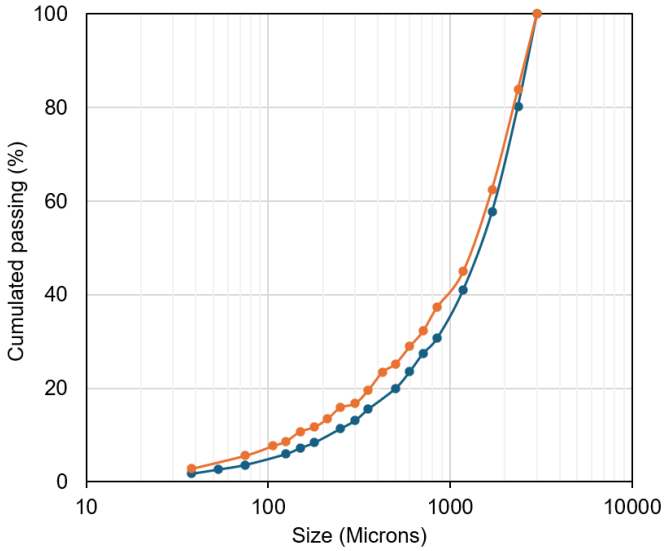

Figure 1. Size analysis for two random charges.

2.2 Batch flotation

Preliminary tests (F1, F2, F3) began by scrubbing a 2 kg charge in the float cell under neutral conditions, after which the slurry was rinsed into a 16 L cylinder for desliming. In the cylinder, the slurry was agitated and allowed to settle, and the water was siphoned off down to the settled solids; this cycle was repeated three times. The deslimed material was then returned to the float cell at 35% pulp density and conditioned at pH 10.5 with 75 g/t Armac T (F1, F2 and F3) as the collector for mica flotation. The frother (3 drops of MIBC) was added, air was introduced and the impeller speed was raised to 2100 RPM, with the froth scraped into a tray. A second dose of Armac T at 25 g/t (F2 and F3) was then added for scavenger flotation, with the froth collected in a second tray. The pulp was subsequently thickened to about 50% pulp density, conditioned with 250 g/t F100 (dispersant) at pH 11 and 1500 RPM, and deslimed again. For montebrasite flotation, the slurry was returned to 35% pulp density in the flotation cell, adjusted to pH 10.5, and conditioned at 1800 RPM with 150 g/t fatty acids (FA2, consisting of oleic and linoleic acids) before rougher flotation. A further 150 g/t of FA2 was added for scavenger flotation at the same pH in F1, while this scavenger dose was reduced to 75 g/t in F2 and F3. Following montebrasite flotation, another F100 conditioning and desliming cycle prepared the material for spodumene flotation in a 1 kg flotation cell. The residual sample underwent high-density conditioning at 60% solids and pH 11 (adjusted with NaOH), using 375 g/t of FA2 for the rougher stage. We then carried out spodumene flotation at 35% solids and pH 8.5, adjusted with Na_2CO_3. Changing the pH modifier from NaOH to Na_2CO_3

did not affect the behavior of fatty acid collectors in aqueous solutions [14]. Therefore, the effect would rather be on the mineral surfaces and, therefore, separation performance. For the scavenger flotation, 150 g/t of FA2 was used. After spodumene flotation, we dried different products, including the tailings (mainly quartz and feldspars), before sending them to SGS for chemical assay. The flowsheet is presented in Figure 2.

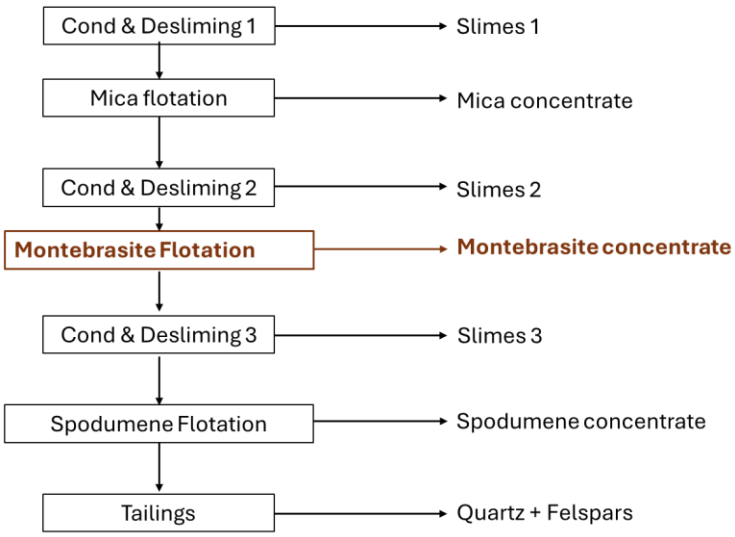

Figure 2. Initial flowsheet for montebrasite flotation from the Moose II deposit

After successfully removing mica, all remaining original charges were dispersed and deslimed, then recombined to form a new bulk sample. The bulk sample was then split into 1 kg charges for further experiments designed to optimize selective flotation of montebrasite. We carried out a new set of preliminary tests to select the best conditions for montebrasite flotation. Of all the tests carried out, we selected one (MoSF4) for chemical assay because it showed fewer spodumene grains in the montebrasite flotation concentrate under the microscope. Design of experiments was then carried out to optimize the Na_2CO_3 and pH for selective montebrasite separation from spodumene.

2.3 Response Surface Modeling (RSM)

RSM is a widespread Design of Experiments (DOE) methodology. Design of experiments is an effective process derived from statistical modeling that allows optimization of experimental tests both in scientific research and in industry [15]. In this study, the Python Statsmodels library (version 0.14.1) [16] was used for the design of experiment methodology, with the purpose of

optimizing the process. Because the variables in our experiments are rather continuous, second-degree plans are used to model the surface response. Among the available second-degree response surfaces/design of experiments, the central composite design (CCD) with three central points was selected for this study to capture curvature in our models, and it allows us to easily identify flat spots from the diagram. Two variables, pH (coded x_1) and Na_2CO_3 dosage (coded x_2), were considered in this study, with corresponding values and levels presented in Table 1. Maximum and minimum values selected for both variables were based on preliminary tests. All pH values were selected at 9.5 and above, as spodumene flotation performs best around pH 8.5, which we are avoiding. Na_2CO_3 dosage was selected after preliminary tests on the dosage effect on the solution during conditioning: above 1350 g/t, dosage did not affect solution pH.

Table 1. Variables and corresponding levels

Level	x_1 = pH	x_2 = Na_2CO_3 (g/t)
-1	9.5	50
0	10.5	700
1	11.5	1350

The flotation tests were performed to recover montebrasite to the concentrate while rejecting spodumene to the tailings. Since montebrasite contains phosphorus but spodumene does not, and spodumene contains silicon but montebrasite does not [10], we evaluated the separation by recoveries of P_2O_5 and SiO_2 to the concentrate, as measures of montebrasite and silicates (especially spodumene), respectively. We used statistical analysis to quantify how pH and Na_2CO_3 dosage affect P_2O5 and SiO_2 recoveries, concentrate grade, and selective separation, and to identify conditions that maximize P_2O_5 recovery while minimizing SiO_2 recovery.

In addition to the recoveries measured, two other responses were calculated: the Gaudin selectivity index, SI (Equation 1) and separation efficiency (SE = P_2O_5 – SiO_2). The Gaudin separation index accounts for both recovery to the concentrate and loss to the tailings [17–19], in our case selectivity between montebrasite and silicate minerals, including spodumene.

$$SI = \sqrt{\frac{P_2O_5 \times (100 - SiO_2)}{SiO_2 \times (100 - P_2O_5)}} \qquad (1)$$

3 Results

3.1 Sample characterization

Assay data from EMPA-LA-ICP-MS showed a head grade of 2.72% Li_2O for the bulk sample, while modal mineralogy data from TIMA-X indicated mainly a mineralogical composition (Figure 3) dominated by spodumene (7.25%), montebrasite (24.5%), quartz (34.7%), albite (24.5%), muscovite (4.51%), apatite (1.22 %), K-feldspars (1.7 %). Mineral liberation analysis indicated that all lithium minerals were fully liberated, with liberation ratio values of 95.8%, 97.5%, 96.9%, 82.8%, and 54.5%, respectively, for spodumene, montebrasite, quartz, albite, and muscovite (Figure 4). It has to be noted that this sample was a composite sample, and thus different from a natural lithium ore from LCT pegmatite, in which montebrasite is minor compared to spodumene.

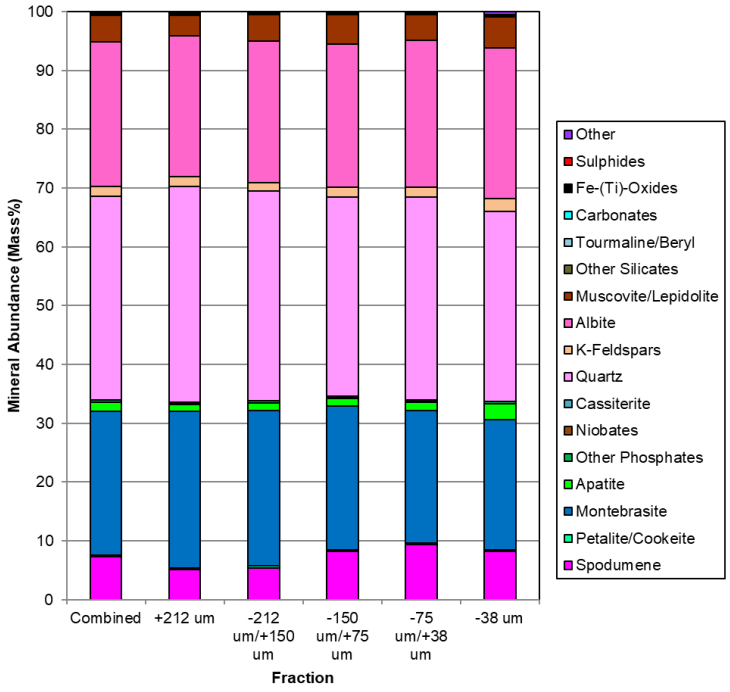

Figure 3. Mineralogical composition for the bulk composite sample from the Moose II deposit

Electron microprobe and laser ablation analysis of 30 points showed that spodumene was of low iron content (< 0.32% Fe_2O_3), with an average of 7.2% Li_2O vs. 8.03% theoretical content. Montebrasite, on the other hand, showed an average of 10.10% Li_2O vs. 10.21% theoretical value, along with a low fluorine content (< 2.30% F), confirming the mineral is rather montebrasite, not amblygonite.

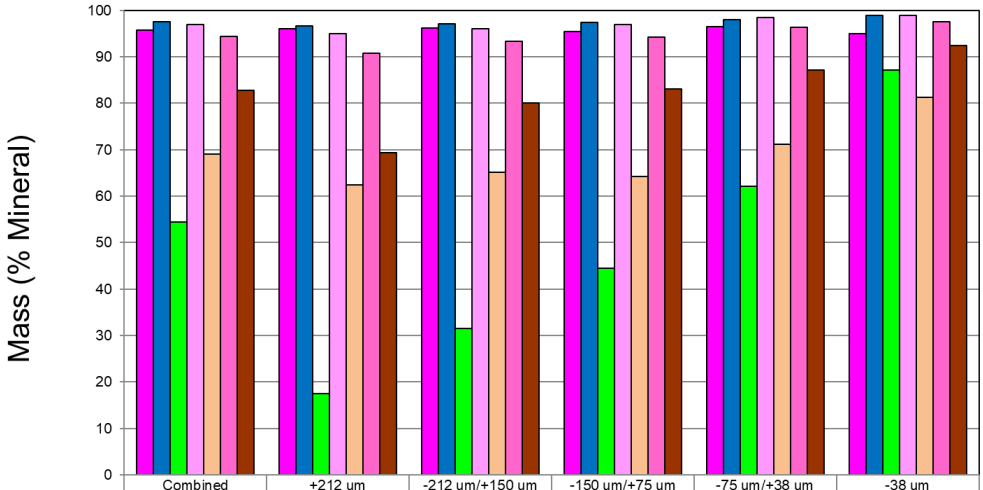

	Combined	+212 um	-212 um/+150 um	-150 um/+75 um	-75 um/+38 um	-38 um
Spodumene	95.8	96.0	96.2	95.5	96.5	95.0
Montebrasite	97.5	96.6	97.1	97.3	98.0	99.0
Apatite	54.5	17.5	31.5	44.5	62.2	87.2
Quartz	96.9	95.0	96.1	97.0	98.4	99.0
K-Feldspars	69.0	62.5	65.1	64.2	71.2	81.2
Albite	94.3	90.8	93.4	94.3	96.3	97.6
Muscovite/Lepidolite	82.8	69.4	80.0	83.1	87.1	92.4

Figure 4. Mineral liberation analysis for the bulk composite sample from the Moose II deposit

3.2 Batch flotation

The recoveries of P_2O_5, Li_2O, and SiO_2 are presented in Figure 5 for all the scoping tests. Selective flotation performance of montebrasite vs. spodumene and gangue minerals was assessed based on the three oxides, since montebrasite was the major P-bearing mineral, except for minor apatite. Similarly, spodumene was the only major silicate mineral floatable with fatty acid collectors. Because both minerals were major lithium-bearing minerals, Li_2O was also used. The ideal conditions for selective montebrasite flotation would therefore maximize P_2O_5 while minimizing SiO_2.

The results indicate that all three preliminary tests on the ore as received (F1, F2, and F3) provided high recoveries of Li_2O (70.42 to 71.86 %) and P_2O_5 (78.91 to 82.04%), while producing minimum recoveries of SiO_2 (3.95 to 5.51%). Since SiO_2 is the main penalty in montebrasite concentrate, test F2 was considered the best performing. The presence of SiO_2 in montebrasite concentrate was attributed to the limited floatability of spodumene before surface pretreatment via high-density conditioning.

Conditions used in F2 were then selected for mica removal from all the 2 kg charges; each product was dispersed and deslimed after high-density conditioning. All charges were then recombined

and split into 1 kg charges for the optimization study; before that, three random charges were subjected to particle size analysis to verify material homogeneity. Before the optimization study, preliminary tests were conducted, and it was observed that spodumene had a tendency to float together with montebrasite since it was subjected to alkaline pretreatment during desliming. Among the different tests that were tried, one of them (MoSF4) provided better separation performance with much lower FA2 dosages (155 g/t). Although montebrasite concentrate of MoSF4 achieved P_2O_5 and Li_2O recoveries of 84.76 and 72.23%, respectively, SiO_2 recovery reached 11.3%, demonstrating the detrimental effect of running high-density alkaline conditioning before montebrasite is removed [9,10].

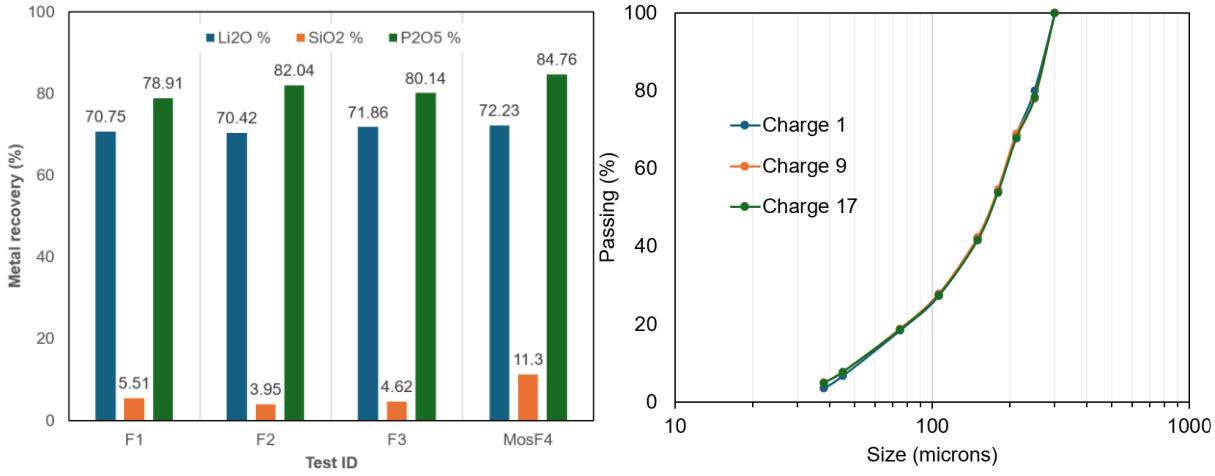

Figure 5. a. Recovery of P_2O_5, Li_2O, and SiO_2 from the preliminary flotation of montebrasite, b. Particle size distribution of the charges prepared for optimization study.

3.3 Response surface analysis

3.3.1 Raw data

The experimental recoveries and the calculated selectivity measures are presented in Table 2 for the eleven runs. Recoveries were lower than in the scoping tests (F1–F3) and MoSF4 because a lower FA2 dosage (125 g/t) was used to limit the flotation of spodumene, whose surface had already been activated by alkaline dispersion at pH 11 during desliming (Section 3.2). This reduced montebrasite recovery but lowered SiO_2 recovery to 2.14% at the selected optimum, compared with 11.3% for MoSF4. These data were used for subsequent modeling in this study. SiO_2 recovery spans almost an order of magnitude (1.67–13.68%), and its variability increases with its level, which violates the constant-variance assumption of least squares; the logarithm is the standard

variance-stabilizing transformation for such responses [20,21]. In Section 3.3.2, we therefore modeled SiO_2 recovery on the natural-logarithm scale, $\ln(SiO_2)$. All SiO_2 predictions are back-transformed to the original scale for presentation and optimization.

Table 2. Experimental design, measured recoveries, and derived selectivity measures.

pH	Na_2CO_3 (g/t)	x_1	x_2	Li_2O (%)	P_2O_5 (%)	SiO_2 (%)	SI	SE (%)
9.5	1350	-1	1	50.11	56.49	2.14	7.71	54.35
10.5	700	0	0	35.54	39.14	2.49	5.02	36.65
11.5	1350	1	1	29.24	30.65	7.90	2.27	22.75
10.5	700	0	0	32.11	35.11	3.23	4.03	31.88
10.5	700	0	0	28.90	31.22	3.10	3.77	28.12
9.5	700	-1	0	63.59	66.69	4.27	6.70	62.42
10.5	50	0	-1	21.61	23.44	2.35	3.57	21.09
10.5	1350	0	1	33.65	36.73	1.67	5.85	35.06
9.5	50	-1	-1	36.83	40.26	2.67	4.96	37.59
11.5	700	1	0	24.18	25.54	7.80	2.01	17.74
11.5	50	1	-1	31.53	32.86	13.68	1.76	19.18

Before modeling, we plotted the raw data against the variables to show the main trend before any model is fitted (Figure 6). It can be seen that Li_2O and P_2O_5 recoveries are highest at pH 9.5 (37–64% Li_2O, 40 – 67% P_2O_5) and fall sharply by pH 10.5. SiO_2 stays low up to pH 10.5 and rises steeply at pH 11.5, reaching 13.7% at the lowest Na_2CO_3 dosage. The plot of the three central points, as repeated, is also included to assess the repeatability. This indicates that lower pH and higher Na_2CO_3 dosage favor selectivity, since we sought to minimize SiO_2.

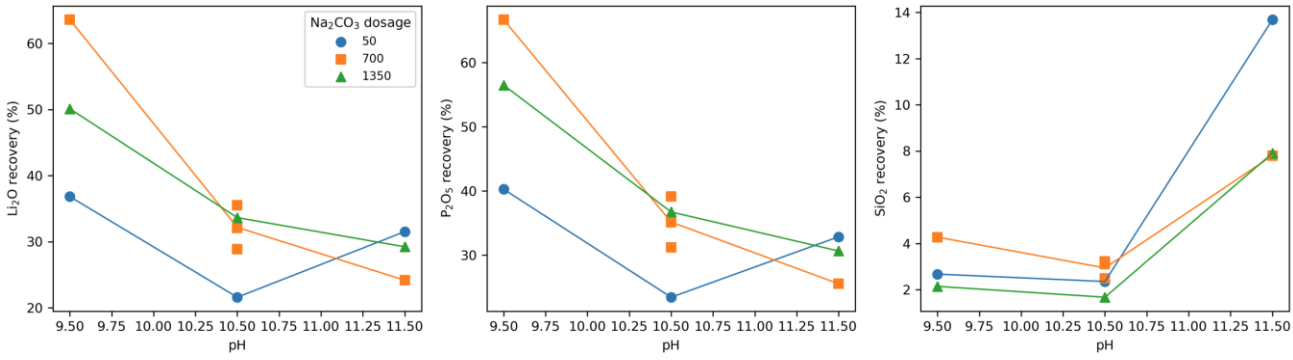

Figure 6. Experimental data of metal recoveries with pH and Na_2CO_3 dosages.

Lithium is the economic product, but it is present in both montebrasite and spodumene, so its recovery cannot distinguish between the two minerals. Plotting Li_2O and P_2O_5 (Figure 7) recoveries against each other shows an almost perfect correlation ($r = 0.996$), while SiO_2 is only

weakly and negatively correlated with either (-0.202 and -0.253, respectively). This establishes that lithium follows phosphorus, since lithium reports to the concentrate with phosphorus. This is mineralogically meaningful, as it is consistent with montebrasite floating and spodumene being rejected. Including Li_2O in the multi-response optimization would also give montebrasite recovery a double weight. Li_2O recovery is therefore reported as measured (Table 2 and Figure 6) and, where needed, estimated from its correlation to P_2O_5.

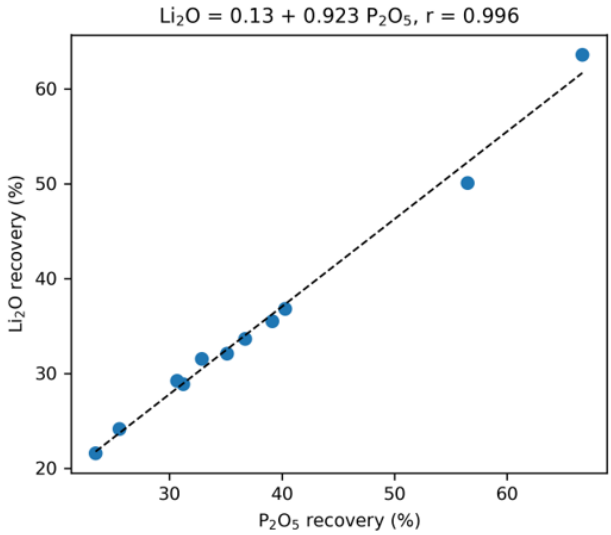

Figure 7. Correlation between Li_2O and P_2O_5 in the montebrasite concentrate (r = 0.996).

3.3.2 Modeling results

The fit statistics of the four models are summarized in Table 3. All four models are statistically significant ($p \leq 0.038$), and none shows significant lack of fit ($p \geq 0.17$), so each quadratic model describes its response within the limits of the experimental error. The models differ, however, in their predictive ability. The Gaudin selectivity index has an excellent model ($R^2 = 0.965$, R^2pred = 0.861, p = 0.001, lack of fit p = 0.81) and is the only response whose model can be relied on to predict untested conditions. The ln(SiO_2) and separation-efficiency models have good explanatory power ($R^2 = 0.92$) but moderate predictive ability (R^2pred = 0.307 and 0.264). The P_2O_5 model explains 85% of the variation but has a negative predicted R^2 (−0.39), which means it describes the measured data but should not be used to predict new conditions.

Table 4. Fit statistics for response surface models

Response	R^2	R^2_{pred}	RMSE	F (model)	p (model)	p (lack of fit)
P_2O_5	0.853	-0.390	7.010	5.82	0.038	0.185
$\ln(SiO_2)$	0.924	0.307	0.256	12.16	0.008	0.174
SI	0.965	0.861	0.510	27.72	0.001	0.811
SE	0.915	0.264	5.904	10.79	0.010	0.297

The coefficients of all models, with their standard errors, t-values, and p-values, are given in Table 4. The data show that pH is the dominant factor for every response, as it is the only significant term for P_2O_5 recovery ($p = 0.008$), with a borderline quadratic term ($p = 0.064$). For $\ln(SiO_2)$, both the linear ($p = 0.002$) and the quadratic ($p = 0.004$) pH terms are significant, which reflects the curved, U-shaped dependence of SiO_2 recovery on pH. Na_2CO_3 has no significant effect on either recovery ($p = 0.17$ for P_2O_5 and 0.14 for $\ln(SiO_2)$), but its effects have opposite signs: it tends to increase P_2O_5 recovery (+4.6) and to decrease SiO_2 recovery (−0.19 on the log scale, about 17% lower SiO_2 recovery from the center to the upper dosage). Because the Gaudin index combines both, these two individually non-significant tendencies add up to a significant effect of Na_2CO_3 on selectivity (+0.92, $p = 0.007$), alongside the strong effect of pH (−2.22, $p < 0.001$). The separation efficiency depends significantly on pH only ($p = 0.001$), with Na_2CO_3 just outside the significance level ($p = 0.064$). No interaction term is significant in any model.

Table 4. Coefficients of the quadratic models in coded units, with standard errors and p-values.

Response	Term	Coefficient (coded)	Std error	t	p-value
P_2O_5	Intercept	35.363	3.596	9.83	< 0.001
	pH	-12.398	2.862	-4.33	0.007
	Na_2CO_3	4.552	2.862	1.59	0.173
	pH × Na_2CO_3	-4.610	3.505	-1.32	0.245
	pH^2	10.443	4.404	2.37	0.064
	$[Na_2CO_3]^2$	-5.587	4.404	-1.27	0.260
ln(SiO_2)	Intercept	1.021	0.131	7.78	< 0.001
	pH	0.590	0.104	5.65	0.002
	Na_2CO_3	-0.185	0.104	-1.77	0.136
	pH × Na_2CO_3	-0.082	0.128	-0.64	0.550
	pH^2	0.808	0.161	5.03	0.004
	$[Na_2CO_3]^2$	-0.261	0.161	-1.62	0.165
SI	Intercept	4.401	0.262	16.81	< 0.001
	pH	-2.220	0.208	-10.66	< 0.001
	Na_2CO_3	0.924	0.208	4.43	0.007
	pH × Na_2CO_3	-0.559	0.255	-2.19	0.080
	pH^2	-0.240	0.321	-0.75	0.487
	$[Na_2CO_3]^2$	0.110	0.321	0.34	0.746
SE	Intercept	32.737	3.029	10.81	< 0.001
	pH	-15.782	2.410	-6.55	0.001
	Na_2CO_3	5.717	2.410	2.37	0.064
	pH × Na_2CO_3	-3.298	2.952	-1.12	0.315
	pH^2	6.563	3.709	1.77	0.137
	$[Na_2CO_3]^2$	-5.442	3.709	-1.47	0.202

3D response surfaces for metal recoveries and selectivity are presented in Figure 8, with experimental design points on top. P_2O_5 recoveries reach a peak at pH 9.5, with Na_2CO_3 above 1350 g/t. SiO_2 recovery passes through a minimum at intermediate pH and rises sharply towards pH 11.5. This is a major argument supporting not probing pH below 9.5, as spodumene starts to float, and not too high a pH, as spodumene starts to be activated by metal cations present in process water [22]. Selectivity plots show improvement steadily as pH decreases and Na_2CO_3 dosage increases, reaching maximum values at pH 9.5 and Na_2CO_3 around 1350 g/t. The central result of this study concerns selectivity. The key finding using the Gaudin selectivity index is that Na_2CO_3 has no significant effect on how much montebrasite or silicate is recovered to the concentrate, but it does significantly improve how cleanly the two are separated.

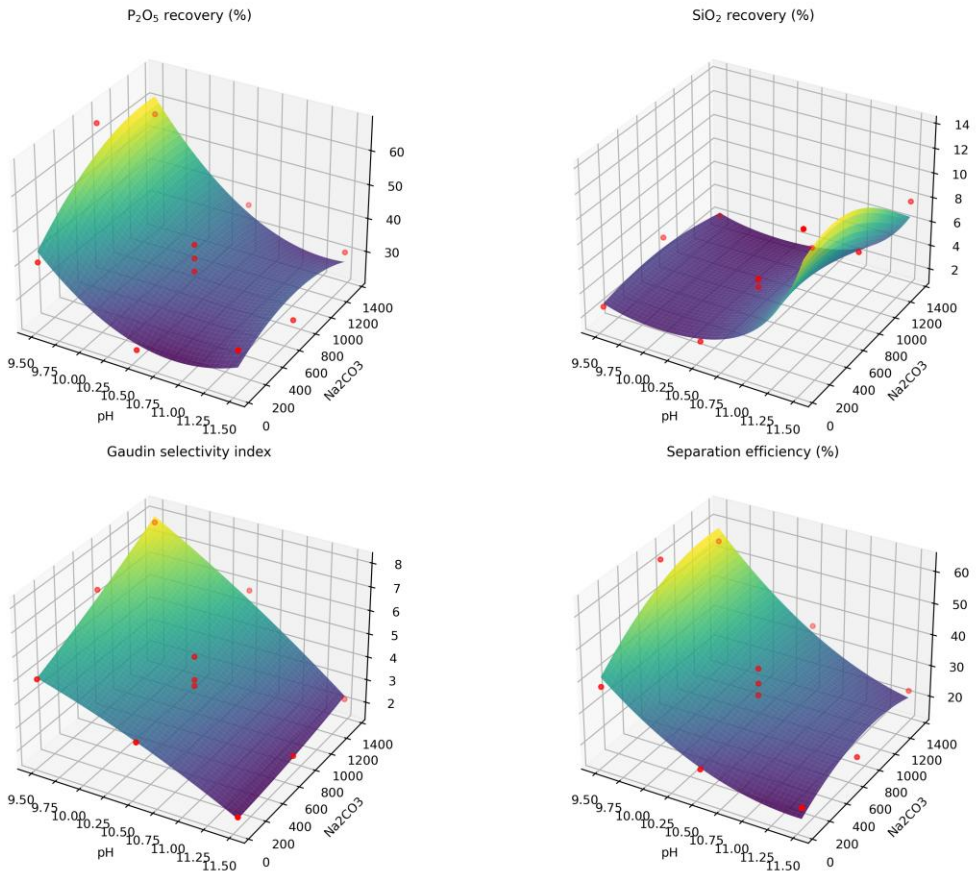

Figure 8. 3D response surfaces of P_2O_5 recovery, SiO_2 recovery (back-transformed), Gaudin selectivity index, and separation efficiency

The overall desirability is highest, D = 0.91, at pH 9.5 and 1350 g/t Na_2CO_3, with individual desirability values of 0.89 for P_2O_5 recovery and 0.94 for SiO_2 rejection. This point coincides with the maximum of the Gaudin index, so the optimization and the selectivity analysis identify the same conditions independently.

The operating window is more useful than the single optimum: desirability stays within 5% of its maximum for pH 9.50 – 9.62 and Na_2CO_3 dosages of about 930–1350 g/t. The prediction profiles through the optimum (Figure 9) show the asymmetry between the two factors: all responses change steeply with pH but only gradually with Na_2CO_3.

All four analyses, including the raw data, the selectivity models, the desirability optimization, and the measured run at the optimum, point to the same operating conditions: the lowest pH and the highest Na_2CO_3 dosage tested. The convergence of independent lines of evidence strengthens the

conclusion beyond what any single model can provide, given the moderate predictive ability of the recovery models.

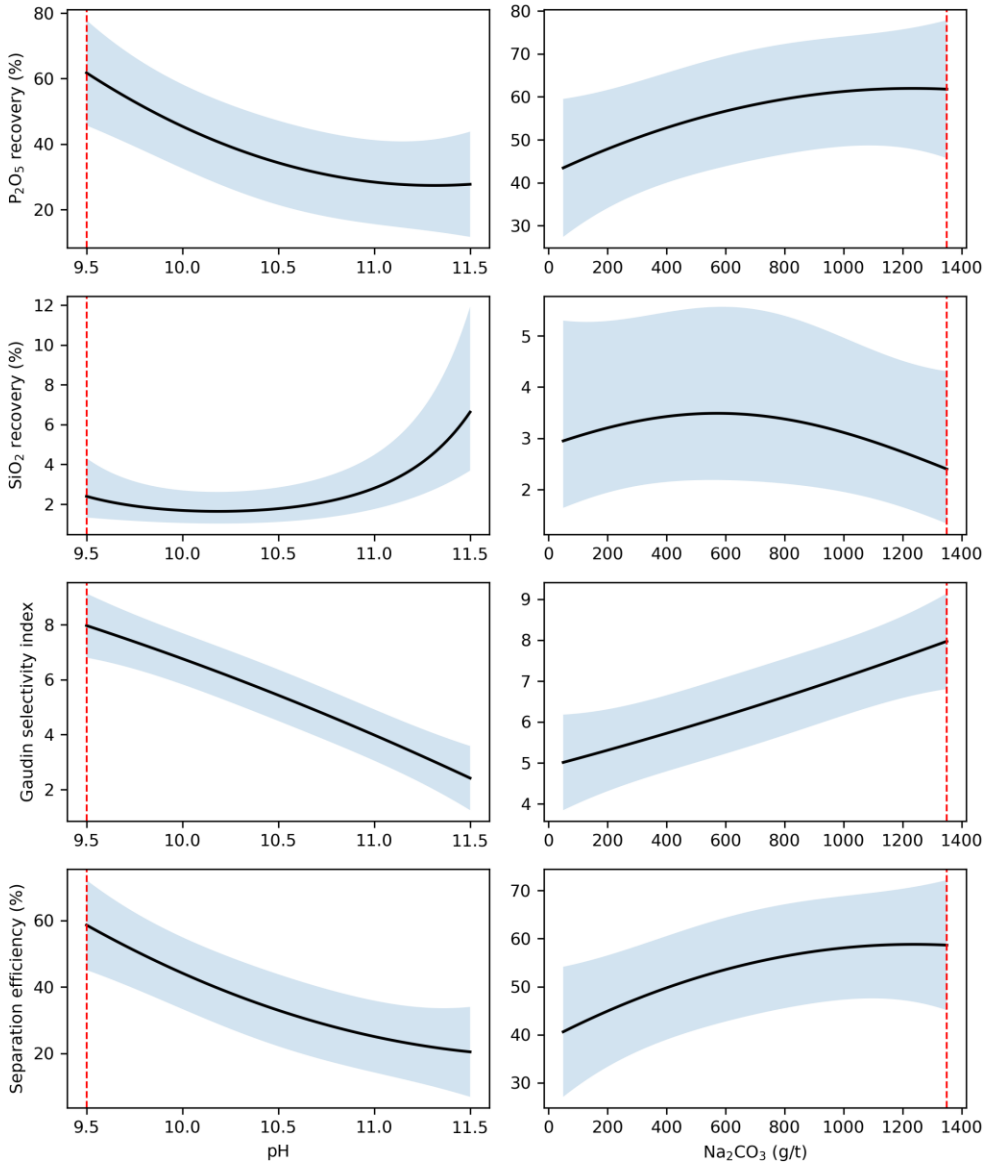

Figure 10. Prediction profiles through the optimum along pH and Na_2CO_3 dosage, with 95% confidence bands. The red line marks the optimum.

References

1. Opoku, P.A.; Tadesse, B.; Albijanic, B.; Nikoloski, A.N. An Overview of Coarse Particle Beneficiation of Lithium Ores. *Scientific Reports* **2025**, *15*, 29091, doi:10.1038/s41598-025-14059-z.

2. Korbel, C.; Filippova, I.V.; Filippov, L.O. Froth Flotation of Lithium Micas – A Review. *Minerals Engineering* **2023**, *192*, 107986, doi:10.1016/j.mineng.2022.107986.
3. Sahoo, S.K.; Tripathy, S.K.; Nayak, A.; Hembrom, K.C.; Dey, S.; Rath, R.K.; Mohanta, M.K. Beneficiation of Lithium Bearing Pegmatite Rock: A Review. *Mineral Processing and Extractive Metallurgy Review* **2024**, *45*, 1–27, doi:10.1080/08827508.2022.2117172.
4. Anderson, M.O. Evolution and Mineralization of the Moose II Lithium-Tantalum Pegmatite Deposit, Northwest Territories, Canada. MSc., University of New brunswick, 2013.
5. Kundu, T.; Rath, S.S.; Das, S.K.; Parhi, P.K.; Angadi, S.I. Recovery of Lithium from Spodumene-Bearing Pegmatites: A Comprehensive Review on Geological Reserves, Beneficiation, and Extraction. *Powder Technology* **2023**, *415*, 118142, doi:10.1016/j.powtec.2022.118142.
6. Burt, R.O.; Flemming, J. Spodumene Processing at Tanco. In Proceedings of the 18th Canadian Mineral Processors Operators Conference; Ottawa, January 1986.
7. Hu, D.; Ma, B.; Lv, Y.; Zhao, Q.; Wang, C.; Chen, Y. A Sustainable Process for Efficient Extraction of Lithium, Aluminum, and Phosphorus from Montebrasite. *ACS Sustainable Chem. Eng.* **2024**, doi:10.1021/acssuschemeng.3c05536.
8. Murhula, E.M.; Wang, W.; Lambiv Dzemua, G.; Lim, S.G.; Schatte, G.; Zuin, L.; Gibson, C.E. Unveiling the Amphoteric Surface Reactivity of Montebrasite Using Spectroscopic and First-Principles Methods. *J. Phys. Chem. C* **2025**, *129*, 17846–17861, doi:10.1021/acs.jpcc.5c04541.
9. Moon, K.S.; Fuerstenau, D.W. Surface Crystal Chemistry in Selective Flotation of Spodumene (LiAl[SiO3]2) from Other Aluminosilicates. *International Journal of Mineral Processing* **2003**, *72*, 11–24, doi:10.1016/S0301-7516(03)00084-X.
10. Murhula, E.M.; Gibson, C.E.; Wang, W.; Babedi, L.; Ng, J.L.; Lim, S.G. Atomic-Scale Insights into the Surface Chemistry, Surface Stability, and Floatability of Spodumene and Montebrasite with Fatty Acid Collectors. *ChemRxiv 2026*, doi:10.26434/chemrxiv.15010231/v1.
11. Filippov, L.; Farrokhpay, S.; Lyo, L.; Filippova, I. Spodumene Flotation Mechanism. *Minerals* **2019**, *9*, 372, doi:10.3390/min9060372.
12. Wang, Y.; Zhu, G.; Zhang, L.; Lu, D.; Wang, L.; Zhao, Y.; Zheng, H. Surface Dissolution of Spodumene and Its Role in the Flotation Concentration of a Spodumene Ore. *Minerals Engineering* **2018**, *125*, 120–125, doi:10.1016/j.mineng.2018.06.002.
13. Xu, L.; Hu, Y.; Tian, J.; Wu, H.; Yang, Y.; Zeng, X.; Wang, Z.; Wang, J. Selective Flotation Separation of Spodumene from Feldspar Using New Mixed Anionic/Cationic Collectors. *Minerals Engineering* **2016**, *89*, 84–92, doi:10.1016/j.mineng.2016.01.013.
14. Murhula, E.M.; Arellano, A.; Cook, B.K.; Gibson, C.E. Effect of (De-)Protonation on the UV Spectra of Sodium Oleate: Experimental and Electronic Structure Investigation. *ACS Appl. Opt. Mater.* **2023**, *1*, 1350–1359, doi:10.1021/acsaom.3c00125.
15. Goupy, J. LES PLANS D'EXPERIENCES. *Revue MODULAD* **2006**, *34*, 43.
16. Seabold, S.; Perktold, J. Statsmodels: Econometric and Statistical Modeling with Python. In Proceedings of the 9th Python in Science Conference; 2010.
17. Mensah, R.; Hsia, T.; Amani, P.; Thang, S.H.; Firouzi, M. Reverse Flotation of Hematite Using a Novel Bio-Collector Derived from Vitamin E. *Minerals Engineering* **2026**, *248*, 110578, doi:10.1016/j.mineng.2026.110578.
18. Oliveira, G.L.; Silva, G.R. da Study of New Commercial Collectors for the Recovery of Coarse Quartz Particles in Iron Ore Flotation. *Physicochem. Probl. Miner. Process.* **2023**, *59*, doi:10.37190/ppmp/174292.
19. Irannajad, M.; Nuri, O.S.; Allahkarami, E. A New Approach in Separation Process Evaluation. Efficiency Ratio and Upgrading Curves. *Physicochem. Probl. Miner. Process.* **2018**, *54*, 847–857, doi:10.5277/ppmp1886.

20. Box, G.E.P.; Cox, D.R. An Analysis of Transformations. *Royal Statistical Society. Journal. Series B: Methodological* **1964**, *26*, 211–243, doi:10.1111/j.2517-6161.1964.tb00553.x.
21. Montgomery, D.C. *Design and Analysis of Experiments*; EMEA Edition, 9th Edition.; Wiley, 2020; ISBN 978-1-119-63842-1.
22. Murhula, E.M.; Wang, W.; Hill-Svehla, C.; Lambiv Dzemua, G.; Babedi, L.; Gibson, C.E. The Role of Na2CO3 in the Selective Flotation of Ca-Activated Spodumene and Quartz. *Minerals Engineering* **2026**, *248*, 110618, doi:10.1016/j.mineng.2026.110618.